



HAL
open science

Microclimate reveals the true thermal niche of forest plant species

Stef Haesen, Jonathan Lenoir, Eva Gril, Pieter de Frenne, Jonas Lembrechts, Martin Kopecký, Martin Macek, Matěj Man, Jan Wild, Koenraad van Meerbeek

► **To cite this version:**

Stef Haesen, Jonathan Lenoir, Eva Gril, Pieter de Frenne, Jonas Lembrechts, et al.. Microclimate reveals the true thermal niche of forest plant species. *Ecology Letters*, 2023, 10.1111/ele.14312 . hal-04239469

HAL Id: hal-04239469

<https://u-picardie.hal.science/hal-04239469v1>

Submitted on 31 Oct 2024

HAL is a multi-disciplinary open access archive for the deposit and dissemination of scientific research documents, whether they are published or not. The documents may come from teaching and research institutions in France or abroad, or from public or private research centers.

L'archive ouverte pluridisciplinaire **HAL**, est destinée au dépôt et à la diffusion de documents scientifiques de niveau recherche, publiés ou non, émanant des établissements d'enseignement et de recherche français ou étrangers, des laboratoires publics ou privés.

1
2
3 **1 Microclimate reveals the true thermal niche of forest plant species**

4
5
6 2 Running title – Incorporating microclimate into SDMs

7
8 3 **Stef Haesen^{1,2}, Jonathan Lenoir³, Eva Gril³, Pieter De Frenne⁴, Jonas J. Lembrechts⁵, Martin**
9
10 4 **Kopecký^{6,7}, Martin Macek⁶, Matěj Man^{6,8}, Jan Wild^{6,9}, Koenraad Van Meerbeek^{1,2}**

11
12 5 *¹Department of Earth and Environmental Sciences, Celestijnenlaan 200E, 3001 Leuven, Belgium; ²KU*
13
14 6 *Leuven Plant Institute, KU Leuven, Leuven, Belgium; ³UMR CNRS 7058 « Ecologie et Dynamique des*
15
16 7 *Systèmes Anthropisés » (EDYSAN), Université de Picardie Jules Verne, Amiens, France; ⁴Forest & Nature*
17
18 8 *Lab, Department of Environment, Ghent University, Geraardsbergsesteenweg 267, 9090 Melle-*
19
20 9 *Gontrode, Belgium; ⁵Research Group PLECO (Plants and Ecosystems), University of Antwerp, 2610*
21
22 10 *Wilrijk, Belgium; ⁶Institute of Botany of the Czech Academy of Sciences, Zámek 1, CZ-25243, Průhonice,*
23
24 11 *Czech Republic; ⁷Faculty of Forestry and Wood Sciences, Czech University of Life Sciences Prague,*
25
26 12 *Kamýcká 129, CZ-165 21, Prague 6 - Suchdol, Czech Republic; ⁸Department of Botany, Faculty of*
27
28 13 *Science, Charles University, Benátská 2, CZ-128 01 Prague 2, Czech Republic; ⁹ Faculty of Environmental*
29
30 14 *Sciences, Czech University of Life Sciences Prague, Kamýcká 129, CZ, 165 21 Prague 6 - Suchdol, Czech*
31
32 15 *Republic;*

33
34
35
36
37
38
39
40
41
42
43
44
45
46
47
48
49
50
51
52
53
54
55
56
57
58
59
60
16 e-mail & OrcIDs (* = corresponding author)

17 Stef Haesen*: stef.haesen@kuleuven.be - <https://orcid.org/0000-0002-4491-4213> - tel. = +32 16 32 24 67
18 Jonathan Lenoir: jonathan.lenoir@u-picardie.fr - <https://orcid.org/0000-0003-0638-9582>
19 Eva Gril: eva.gril@u-picardie.fr - <https://orcid.org/0000-0002-7340-8264>
20 Pieter De Frenne: pieter.defrenne@ugent.be - <https://orcid.org/0000-0002-8613-0943>
21 Jonas J. Lembrechts: lembrechtsjonas@gmail.com - <https://orcid.org/0000-0002-1933-0750>
22 Martin Kopecký: ma.kopecky@gmail.com - <https://orcid.org/0000-0002-1018-9316>
23 Martin Macek: Martin.Macek@ibot.cas.cz - <https://orcid.org/0000-0002-5609-5921>
24 Matěj Man: Matej.Man@ibot.cas.cz - <https://orcid.org/0000-0002-4557-8768>
25 Jan Wild: Jan.Wild@ibot.cas.cz - <https://orcid.org/0000-0003-3007-4070>
26 Koenraad Van Meerbeek: koenraad.vanmeerbeek@kuleuven.be - <https://orcid.org/0000-0002-9260-3815>

27 **Keywords:** species distribution modelling, habitat suitability modelling, ecological niche models,
28 MaxEnt, microclimate, microrefugia, ForestClim, forest plant species, species response curves,
29 understory temperatures

1
2
3 30 **Article type:** Letter
4

- 5
6 31 • *Word count: abstract (162), main text (5478) consisting of introduction (747), methods (2338),*
7 32 *results (562), discussion (1721), and conclusion (110)*
8
9 33 • *Number of references: 81*
10
11 34 • *Number of figures: 6 in main text, 3 in supporting information*
12
13 35 • *Number of tables: 0 in main text, 3 in supporting information*
14
15 36 • *Number of text boxes: 0 in main text, 0 in supporting information*

16
17 37 **Statement of authorship**

18
19 38 SH, JL, PDF, JLL, and KVM designed the research. SH performed the data analyses, with contributions
20
21 39 from JL, EG, PDF, JLL, MK, MM, MM, JW and KVM. SH wrote the manuscript, with contributions from
22
23 40 JL, EG, PDF, JLL, MK, MM, MM, JW and KVM. All authors contributed substantially to revisions.

24
25 41 **Data accessibility statement**

26
27 42 Code and data are available at <https://figshare.com/s/c25cdebad1474201b733>. The raw biodiversity
28
29 43 data is available at <https://doi.org/10.15468/dl.kf533a>. ForestClim is freely-available at
30
31 44 <https://doi.org/10.6084/m9.figshare.22059125>.

ABSTRACT

Species distributions are conventionally modelled using coarse-grained macroclimate data measured in open areas, potentially leading to biased predictions since most terrestrial species on Earth reside in the shade of trees. Here, we compared conventional macroclimate-based species distribution models (SDMs) with models corrected for forest microclimate buffering, at both coarse and high spatial resolution, for forest plant species across Europe. We show that microclimate-based SDMs at high spatial resolution outperformed models using macroclimate and microclimate data at coarser resolution. Additionally, macroclimate-based models introduced a systematic bias in modelled species response curves, which could result in erroneous range shift predictions under climate change. Critically important for conservation science, these models were unable to identify warm and cold refugia at the range edges of species distributions. Our study emphasizes the crucial role of microclimate data when SDMs are used to gain insights into biodiversity conservation in the face of climate change, particularly given the growing policy and management focus on the conservation of refugia worldwide.

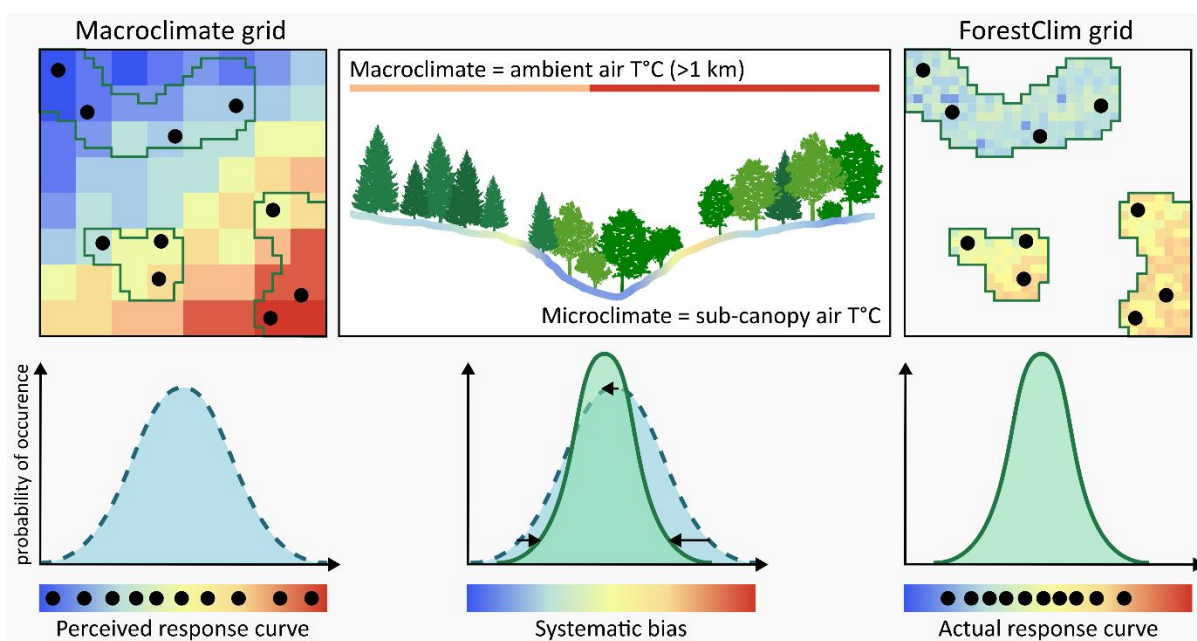
59 INTRODUCTION

60 Over the last decades, species distribution models (SDMs, also known as habitat suitability models or
61 ecological niche models), have emerged as a central method to project the effects of changing
62 environmental conditions on species' distributions in space and time (Booth et al., 2014; Elith &
63 Leathwick, 2009; Guisan & Zimmermann, 2000; Zimmermann et al., 2010). Most SDMs are correlative
64 models that infer relationships between species occurrences and the environment using statistical or
65 machine learning methods (Elith & Leathwick, 2009). Conventional SDM practices involve the
66 incorporation of a standard set of bioclimatic variables with a typical spatial resolution of 30 arc
67 seconds such as in the WorldClim (Fick & Hijmans, 2017) or CHELSA (Karger et al., 2017) datasets.
68 However, these climatological data are derived from standardized meteorological stations at
69 approximately 2 meters height above short grass, exposed to wind, and well away from trees to
70 minimize any noise generated by microclimatic effects (Jarraud, 2008). Gridded macroclimatic data
71 interpolate such weather stations' data and thus represent the free-air temperature conditions in
72 open ecosystems. Although these data are sufficient to adequately capture changes in free-air
73 temperatures, SDMs based on coarse-scale climate data should be expected to introduce a bias, which
74 stems from the simplified assumptions these models make about the causal relationship between
75 spatially-averaged climatic predictors and the fitness of individual organisms or likelihood of persistent
76 populations (Fourcade et al., 2018; Lozier et al., 2009). This might be especially problematic when
77 using these data to model the response curves of species that live close to the ground, in
78 topographically heterogenous terrain, or under trees and shrubs.

79 Variation in microclimates results from physical processes such as airflow and incoming solar
80 radiation that interact with topographic factors such as slope, aspect and surface roughness (Geiger,
81 1950). Additionally, vegetation cover is known to affect local microclimate temperature (De Frenne et
82 al., 2019; Lenoir et al., 2017). Indeed, it is currently well acknowledged that forests harbour distinct
83 microclimatic conditions owing to the structural complexity of the canopy, resulting in shading and
84 evapotranspirative cooling (Geiger, 1950). Forest canopies are characterized by their buffering
85 capacities of extreme temperatures in comparison to weather station data, with cooler sub-canopy
86 maximum temperatures and warmer sub-canopy minimum temperatures (De Frenne et al., 2019). In
87 European forests, this difference can add up to 9°C for mean monthly temperatures (Haesen et al.,
88 2021). There is an urgent need for greater use of fine-scale microclimatic data in ecology as ignoring
89 the mismatch between conventionally-used macroclimatic data and the microclimatic conditions
90 might lead to erroneous predictions, wrong ecological interpretations and, ultimately, questionable
91 conservation decisions (Körner & Hiltbrunner, 2018).

1
2
3 92 This study aims to evaluate the influence of large-scale, gridded microclimate data on the
4 93 accuracy of SDMs and associated environmental niches and projected geographic ranges of European
5 94 plant species constrained to forest habitats. Challenging conventional SDMs, we separately tested the
6 95 effects of using microclimate instead of macroclimate data, as well as of the spatial resolution of these
7 96 data. To achieve this, we employed three types of SDMs using (1) a macroclimatic dataset at a spatial
8 97 resolution of $1 \times 1 \text{ km}^2$; (2) an aggregated microclimatic dataset that matched the resolution of the
9 98 macroclimatic dataset but using sub-canopy microclimate temperatures; and (3) a microclimatic
10 99 dataset with a spatial resolution of $25 \times 25 \text{ m}^2$, matching the species compositional patterns in the
11 100 forest understory vegetation and using the microclimate temperatures as perceived below the canopy
12 101 (Figure 1; Haesen et al., 2023).

13
14
15
16
17
18
19
20 102 Forests are recognized for their capacity to moderate temperature, and as such, plant species
21 103 adapted to forest ecosystems are likely to respond to warmer minimum temperatures and cooler
22 104 maximum temperatures than those estimated by free-air temperature data collected from weather
23 105 stations. Therefore, we hypothesized that (1) the actual thermal response curves of forest specialist
24 106 species are more narrow than the thermal response curve as modelled from gridded macroclimate
25 107 data. We also expect that (2) ranges projected from macroclimate-based models are overestimated,
26 108 because the presence of a species at locations with distinct microclimates compared to their
27 109 surroundings, may be erroneously attributed to the species' ability to survive in the entire area with
28 110 that macroclimate. Finally, assuming that species are constrained by the maximum temperature at
29 111 the southern limit of their latitudinal range and by the minimum temperature at their northern limit,
30 112 we hypothesized that (3) populations of forest specialist species may survive in local microrefugia,
31 113 which are cooler than the surrounding landscape at the southern latitudinal limit but warmer than the
32 114 surrounding area at the northern latitudinal limit.



115

116 *Figure 1: Design of this comparative study, where we compared species distribution models with different set-*
 117 *ups of climatic data. As forests are known to buffer sub-canopy temperatures, forest specialist plant species*
 118 *respond to warmer minimum temperatures and colder maximum temperatures as perceived by the free-air (i.e.*
 119 *macroclimate) temperature data. Therefore, we hypothesize that the actual thermal response curves of forest*
 120 *specialist species, as modelled with the high-resolution ForestClim dataset, would be narrower than the thermal*
 121 *response curve modelled by macroclimate-based SDMs. Note that ForestClim is only available for forest areas,*
 122 *which are delineated by green lines within the simulated grids. Black points indicate species occurrences of a*
 123 *virtual forest plant species (adapted from Lenoir et al., 2017).*

124 **METHODS**

125 **Study area & species selection**

126 Our study area encompasses all 27 EU countries, plus Albania, Andorra, Bosnia and Herzegovina,
127 Kosovo, Liechtenstein, Montenegro, North Macedonia, Norway, San Marino, Serbia, Switzerland and
128 the United Kingdom. The Canary Islands and Azores, as well as Europe's overseas territories were
129 excluded from the analysis.

130 Forest specialist species were selected based on the European forest vascular plant species
131 list (Heinken et al., 2022), which is based on vegetation databases, literature and expert knowledge.
132 From this list, we first selected shrub and herb species, which – unlike tree species – usually complete
133 their entire life cycle within the forest understory layer, thus experiencing forest microclimate
134 dynamics (Caron et al., 2021). Subsequently, we selected the species categorized as forest specialists
135 (i.e., categories 1.1 and 1.2) throughout their entire range, meaning that these species occur only in
136 closed-canopy forests, forest edges or forest openings.

137 **Environmental predictors**

138 Three different sets of bioclimatic temperature-related variables (i.e., macroclimatic data at $1 \times 1 \text{ km}^2$,
139 microclimatic data aggregated at the spatial resolution matching the gridded macroclimate data at 1
140 $\times 1 \text{ km}^2$ and microclimatic data at the native spatial resolution of $25 \times 25 \text{ m}^2$) were used to construct
141 our SDMs, starting from the conventional set of eleven bioclimatic temperature variables. However,
142 we excluded mean temperature of the wettest quarter (BIO8) and mean temperature of the driest
143 quarter (BIO9) as these were recently criticized for their use within species distribution models (Booth,
144 2022). As the available CHELSA and WorldClim data are not fully covering our study period (2000-
145 2020), we used TerraClimate to construct the 'macroclimatic dataset' at the typical spatial resolution
146 of $1 \times 1 \text{ km}^2$ as used in conventional SDMs. However, TerraClimate bioclimatic variables covering the
147 2000-2020 period are available at a spatial resolution of $4 \times 4 \text{ km}^2$ and thus were spatially downscaled
148 to a spatial resolution of $1 \times 1 \text{ km}^2$. To do this, we first calculated, for each $1 \times 1 \text{ km}^2$ grid cell, the
149 difference between the bioclimatic variables of TerraClimate (1970-2000 period) and WorldClim
150 (1970-2000 period) and then added these offset values or anomalies to the TerraClimate bioclimatic
151 variables for the 2000-2020 period to obtain a final macroclimate layer of $1 \times 1 \text{ km}^2$ resolution. This
152 method assumes that the offset values from the long-term average period of 1970-2000 are still valid
153 for the period 2000-2020.

154 The 'microclimatic dataset' consists of the original bioclimatic variables provided within
155 ForestClim, a new high-resolution dataset of forest understory temperature for all European forests

1
2
3 156 at a spatial resolution of $25 \times 25 \text{ m}^2$ derived from the ForestTemp model (Haesen et al., 2021, 2023).
4
5 157 Briefly, ForestTemp was created by combining more than 1,200 time series of *in situ* near-surface
6
7 158 forest temperatures from across Europe with topographical, biological and macroclimatic predictors
8
9 159 in a machine learning model. The ‘aggregated dataset’ was generated by averaging the ForestClim
10
11 160 bioclimatic variables to a $1 \times 1 \text{ km}^2$ resolution. Note that we did not opt to include a high-resolution
12
13 161 macroclimatic dataset (i.e., $25 \times 25 \text{ m}^2$; topographically downscaled) within this comparative study as
14
15 162 this would be representative for topoclimatic conditions, which are proximal as well. However,
16
17 163 topoclimate would not capture the influence of the canopy cover on below-canopy temperatures,
18
19 164 which would turn it into an intermediate ‘mesoclimate’ product, adding extra layers of complexity to
20
21 165 the comparative analyses. Besides, the benefit of using topoclimate over macroclimate in SDMs is
22
23 166 fairly well covered in the scientific literature (Dobrowski, 2011; Man et al., 2022).

24
25 167 Each set of bioclimatic temperature variables was complemented with six bioclimatic
26
27 168 precipitation variables. From the conventional set of eight bioclimatic precipitation variables, we
28
29 169 omitted precipitation of the warmest quarter (BIO18) and precipitation of the coldest quarter (BIO19)
30
31 170 for similar reasons discussed by (Booth, 2022). The six bioclimatic precipitation variables were
32
33 171 calculated from TerraClimate precipitation data for the 2000-2020 period and disaggregated to match
34
35 172 the spatial resolution of each bioclimatic set. Finally, edaphic variables were added, since soil data
36
37 173 often increase model performance (Hageer et al., 2017). Based on their effects on plant demography,
38
39 174 we selected four soil variables: bulk density (bdod; cg/cm^3), which reflects the soil porosity; soil clay
40
41 175 content (clay; g/kg), which reflects the soil texture; pH H_2O (pH; unitless); and cation exchange
42
43 176 capacity (cec; mmol_c/kg ; (Hageer et al., 2017)). The soil raster layers were downloaded from the
44
45 177 SoilGrids 2.0 database (Poggio et al., 2021) at a resolution of 250 m for three different depths: 0-5 cm;
46
47 178 5-15 cm; and 15-30 cm. These three layers were averaged into one single layer representing the depth
48
49 179 from 0 cm to 30 cm, with the exception of soil pH (i.e., a logarithmic scale), which was aggregated
50
51 180 using the median value over the three layers.

52
53 181 To reduce overfitting of SDMs, multicollinearity between the predictors was assessed using a
54
55 182 pairwise Spearman correlation test (Figure S1). Highly correlated variables (Spearman correlation
56
57 183 coefficients > 0.7) were removed from the analysis in order to reach the most parsimonious model
58
59 184 (Dormann et al., 2013). When excluding one of the correlated covariate pair, we preferentially
60
185 retained variables which are known to be more important for plant species distributions (Macek et al.,
186
187 2019). The final selection of covariates encompassed two temperature variables (maximum
188
temperature of the warmest month (BIO5) and minimum temperature of the coldest month (BIO6)),
two precipitation variables (mean annual precipitation, (BIO12) and precipitation seasonality (BIO15))

1
2
3 189 and two edaphic variables (cation exchange capacity and soil clay content). All covariate layers were
4
5 190 projected in an equal-area projection (epsg:3035; ETRS89/LAEA).

191 **Species occurrence data**

192 Georeferenced occurrence data were downloaded from the Global Biodiversity Information Facility
193 on the 13th of September 2022 (<https://doi.org/10.15468/dl.kf533a>). To improve data quality for each
194 species, the occurrence data were filtered in the following sequential steps: (1) only records of ‘human
195 observations’ were selected; (2) records with an unknown coordinate uncertainty or coordinate
196 uncertainty larger than 25 m (i.e., the pixel size) were excluded; (3) records located at country or
197 capital centroids and biodiversity institutions (e.g., botanical gardens) were omitted (Cheng et al.,
198 2021); (4) duplicate records were removed; (5) records outside our study area were deleted; (6) only
199 records observed during our climatic reference period (2000-2020) were selected; (7) records were
200 spatially thinned to one random observation per 25 × 25 m² grid cell; and (8) species with less than 50
201 cleaned occurrence records were omitted, which has been postulated as a minimum standard to build
202 robust SDMs (van Proosdij et al., 2016).

203 Filtering of species occurrence data resulted in a final dataset of 140 species, which are further
204 used for the analyses (Table S1). Note that the same occurrence datasets are needed over the different
205 climatic set-ups to have comparable model outputs. Here, we decided to work with occurrence
206 datasets that underwent a cleaning protocol based upon the characteristics of the microclimatic
207 dataset (i.e., maximum coordinate uncertainty of 25 m, and spatial thinning to a 25 × 25 m² grid cell).

208 **Species distribution modelling**

209 We used MaxEnt, a presence-background algorithm that combines species presence-only data with
210 environmental predictors for the current climate to predict the environmental suitability of each study
211 species across our study area (Phillips et al., 2017). We did that for each of the three sets of bioclimatic
212 variables (i.e., the macroclimatic set, the aggregated microclimatic set and the microclimatic set at the
213 native resolution), thus generating three sets of habitat suitability maps for each study species.
214 Background data were generated by sampling an equal amount of background points as occurrence
215 points (i.e., so that species prevalence equals 50%) based on a 2D kernel-density estimate of the
216 occurrence point (Venables & Ripley, 2002), meaning that the spatial density of the background points
217 is proportional to the spatial density of occurrence points for a given species, thereby accounting for
218 spatial bias in the occurrence points (Lake et al., 2020).

219 Although widely-used in scientific research, MaxEnt could suffer from issues like spatial bias
220 and bad model performance due to overfitting (Radosavljevic & Anderson, 2014). To deal with the

1
2
3 221 problem of spatial bias, we conducted spatially independent evaluations in ENMeval2.0 (Kass et al.,
4 222 2021; Muscarella et al., 2014) using block cross-validation and allocating 80% of our occurrence points
5 223 to this cross-validation procedure (20% is kept for independent evaluation). Furthermore, model
6 224 performance was improved by tuning the model settings in ENMeval2.0 rather than working with the
7 225 default settings of MaxEnt. This was implemented by means of a grid search over the possible values
8 226 of the two hyperparameters: feature classes (Linear, Quadratic, Product) and regularization
9 227 multipliers (0.5, 1, 2, 3, 4 and 5). Linear, quadratic and product features were selected to allow for
10 228 linear and quadratic relationships as well as interactions among predictors (Merow et al., 2013).
11 229 Regularization multipliers, on the other hand, control model complexity and overfitting. The larger
12 230 these regularization multipliers, the smoother the model predictions. Here, we ensured that feature
13 231 classes and regularization multipliers were tuned to limit overfitting and increase model performance
14 232 by using an independent subset of the data (i.e., 20%) not involved in the block cross-validation
15 233 procedure.

234 **Model performance & sensitivity**

235 In order to customize the settings for the feature classes and the regularization multipliers, a total of
236 24 different models were run for every single species. The Akaike Information Criterion (AIC) for small
237 sample sizes (20 % of occurrence points) was used to select the best candidate models (Burnham &
238 Anderson, 2004). Next, model performance was assessed using the Continuous Boyce Index (CBI),
239 instead of the commonly-used area under the receiver-operating characteristic curve (AUC). The latter
240 has recently been shown to be biased in presence-only models and should therefore be avoided
241 (Jiménez & Soberón, 2020). The CBI is a threshold-independent metric that represents the relationship
242 between predicted habitat suitability and the distribution of occurrence records (Hirzel et al., 2006).
243 Additionally, we calculated the sensitivity enabling us to quantify how good our model is able at
244 distinguishing true positives from false negatives. Both were calculated based on the independent
245 20% subset of the data.

246 Finally, we used Bayesian regression models (BRMs) in order to assess differences in model
247 performance and sensitivity between SDMs constructed using the three different sources of climate
248 data. We opted for BRMs as they are able to account for data dependencies (i.e., values clustered
249 within species), unequal variances among groups and skewed distributions. The final model structures
250 are added in Table S2. Both sensitivity and CBI were modelled with a beta distribution. The CBI metric
251 was rescaled between 0 and 1 before analysis. Bayesian regression models were run using the *brms*
252 package (Bürkner, 2021). All models were first run using standard priors and with 2 chains, 10,000
253 iterations and a warm-up of 1000 runs. When models did not converge, the flat priors were replaced

1
2
3 254 by weakly informative priors (Table S2) and the models were run again with 4 chains. The final models
4
5 255 converged with \hat{R} values close to 1 (Gelman and Rubin's diagnostic) and all bulk and tail effective
6
7 256 sample sizes of the means were greater than 2500. When the highest posterior density intervals ($\alpha =$
8
9 257 0.05) of the contrasts, calculated using the *emmeans* package (Lenth, 2021), did not overlap with zero,
10 258 contrasts are considered 'significant'.

11 12 259 **Model predictions**

13
14 260 Habitat suitability was predicted for each species and for each of the three sets of bioclimatic
15 261 temperature variables (macroclimatic, aggregated microclimatic and microclimatic) for the 2000-2020
16 262 period. Furthermore, we transformed the logistic maps (i.e., probability values for habitat suitability)
17 263 to binary (presence-absence) maps using the 10% training presence as a threshold, meaning that the
18 264 suitable area contains 90% of the original occurrence records (Benito et al., 2013).

19
20
21
22
23 265 To compare between model predictions from SDMs constructed with different climate
24 266 sources and resolutions, we calculated both the potential suitable area and the potential latitudinal
25 267 range of each species. To make a valid comparison between the three climate types, we disaggregated
26 268 the binary maps derived from macroclimatic and aggregated data ($1 \times 1 \text{ km}^2$) to the finer resolution
27 269 ($25 \times 25 \text{ m}^2$), and subsequently masked out all non-forest pixels. First, the potential suitable area (km^2),
28 270 for each modelled species, was calculated as the sum of all forest pixels classified as potentially
29 271 suitable under the binary maps. Second, the northern and southern latitudinal limit of the predicted
30 272 distributional ranges were defined as the 95% and 5% quantile in latitudinal position, respectively, of
31 273 all pixels classified as potentially suitable. Next, we quantified species thermal response curves for
32 274 mean annual temperature (BIO1), maximum temperature of the warmest month (BIO5) and minimum
33 275 temperature of the coldest month (BIO6) by extracting the climatic conditions over the entire
34 276 potentially suitable area. To optimize computation power, we randomly sampled 1,000,000 pixels
35 277 over the potentially suitable area for microclimate-based maps. For each variable, we derived the cold
36 278 limit (Q05), the optimum (mode), the warm limit (Q95), and the niche width (Q95 – Q05). Analogous
37 279 to the model performance calculations, we used BRMs with the same settings to assess differences in
38 280 model predictions between the SDMs based on the three types of climate data (Table S2). Values of
39 281 bioclimatic variables were standardized before the analysis to aid model convergence.

40
41
42
43
44
45
46
47
48
49
50
51
52
53 282 Finally, we analyzed whether species are constrained to specific (relative) temperature
54 283 conditions (i.e., here defined as microrefugia) at their northern and southern latitudinal limits, as this
55 284 is important for biodiversity conservation. For the northern and southern latitudinal limit, we
56 285 extracted the 5% most southern and northern occurrence records, respectively. Using paired two-
57 286 sided t-tests ($\alpha = 0.05$), we compared the local temperature conditions of these occurrence points to

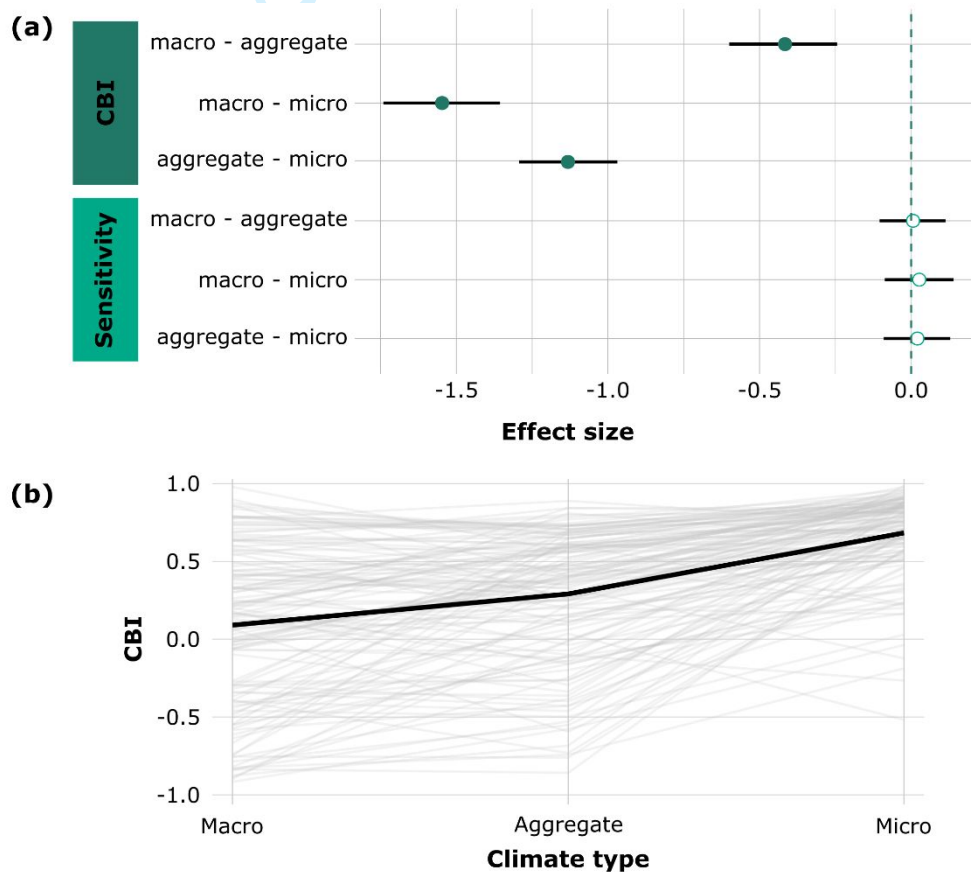
1
2
3 287 the mean surrounding microclimatic conditions over a range of circular buffers (i.e., 100 m, 500 m,
4 288 1000 m, 2500 m, 5000 m; Figure S2) around each occurrence record. A significant t-test implied a
5 289 significant difference in local temperatures at the presence locations as compared with the
6 surrounding area, suggesting that occurrences were restricted to microrefugia.
7
8
9

10 291 All calculations were performed in R version 4.1.1 (R Core Team, 2021). The Tier-2 Genius
11 292 cluster from the high-performance computing facilities of Flanders was used to make the predictions.
12 In order to improve reproducibility, we followed the ODMAP (Overview, Data, Model, Assessment and
13 293 Prediction; Zurell et al., 2020) protocol to report on the SDMs in this study (Table S3).
14
15
16
17
18
19
20
21
22
23
24
25
26
27
28
29
30
31
32
33
34
35
36
37
38
39
40
41
42
43
44
45
46
47
48
49
50
51
52
53
54
55
56
57
58
59
60

For Review Only

295 **RESULTS**296 **Model performance & sensitivity**

297 We found significant differences ($\alpha = 0.05$) in model performance between models constructed with:
 298 (i) macroclimatic (mean CBI = 0.09; se = 0.04) and microclimatic (mean CBI = 0.67; se = 0.02) data; (ii)
 299 macroclimatic and microclimatic data but aggregated at a spatial resolution matching macroclimate
 300 data (mean CBI = 0.28; se = 0.04); and (iii) aggregated microclimatic and microclimatic data at the
 301 native resolution (Figure 2a). For 92% of the species, fine-grained microclimate data systematically
 302 improved model performance (Figure 2b). Here, 39% of macroclimate-based SDMs are characterized
 303 by CBI values smaller than zero, meaning that these models perform worse than random. On the other
 304 hand, CBI values are positive for almost all (96%) microclimate-based SDMs. Furthermore, there were
 305 no significant differences between any of the groups regarding the sensitivity of the models.



306

307 *Figure 2: (a) Pairwise comparison of model performance (quantified as the Continuous Boyce Index, CBI) and*
 308 *sensitivity between SDMs built with macroclimatic, aggregated microclimatic and microclimatic data. A positive*
 309 *effect size of the comparison reflects a higher model performance and sensitivity in SDMs built with the first*
 310 *group of climate data compared to the second group of climate data. Negative effect sizes reflect the opposite*
 311 *result. Points and associated black error bars correspond to posterior means and 95% highest posterior density*
 312 *intervals of the differences (of the scaled CBI and sensitivity). Significant differences are indicated by solid dots*
 313 *whereas non-significant differences are indicated by transparent dots; (b) The performance of each SDM per*
 314 *species (grey lines) over the three types of climate data (i.e., macroclimatic data, aggregated microclimatic data*
 315 *and microclimatic data). The thick black line shows the average CBI value over each of the three climate types.*

Potential suitable area & latitudinal range

The binary distribution maps showed clear differences in the potential suitable area and the potential latitudinal range covered by each species between models calibrated with macroclimatic data and models calibrated with microclimatic data at the native spatial resolution of $25 \times 25 \text{ m}^2$ (e.g., *Paris quadrifolia*; Figure S3). Bayesian regression models confirm these visual interpretations for all modelled species (Figure 3). Relative to microclimate-based SDMs at the native spatial resolution, both the northern and southern limit of the species' latitudinal ranges are significantly overestimated when using either macroclimate-based SDMs or the aggregated version of microclimate-based SDMs. Consequently, species' potential latitudinal ranges are significantly narrower when using SDMs calibrated with microclimatic data (mean = 2,261 km; se = 42 km) in comparison with SDMs calibrated with aggregated microclimatic data (mean = 2,580 km; se = 43 km) or macroclimatic data (mean = 2,620 km; se = 49 km). Analogous, a species' potential suitable area is significantly smaller when using SDMs calibrated with microclimatic data (mean = 911,845 km^2 ; se = 30,383 km^2) in comparison with SDMs calibrated with aggregated microclimatic data (mean = 1,148,763 km^2 ; se = 33,527 km^2) or macroclimatic data (mean = 1,268,189 km^2 ; se = 38,274 km^2).

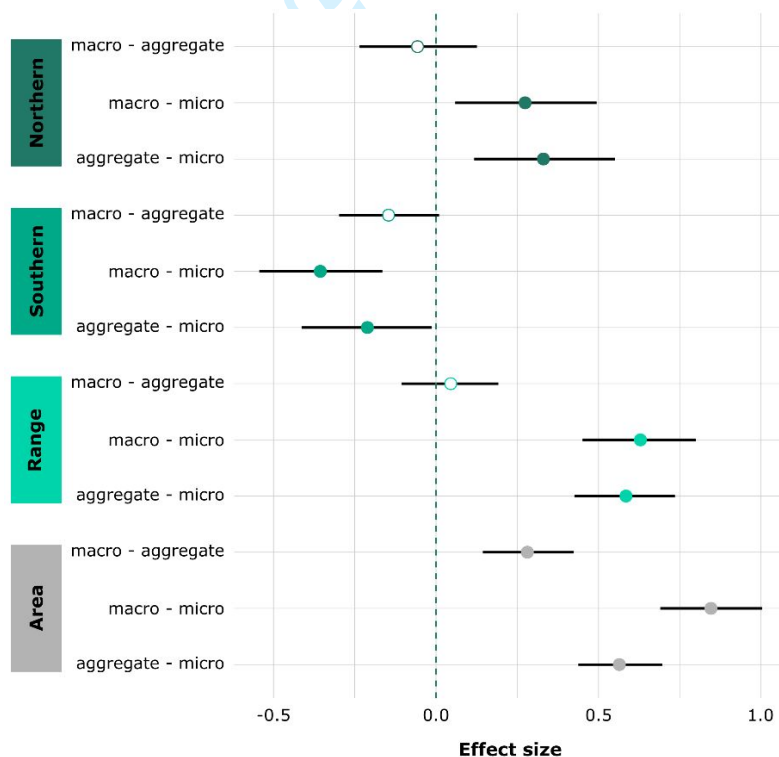
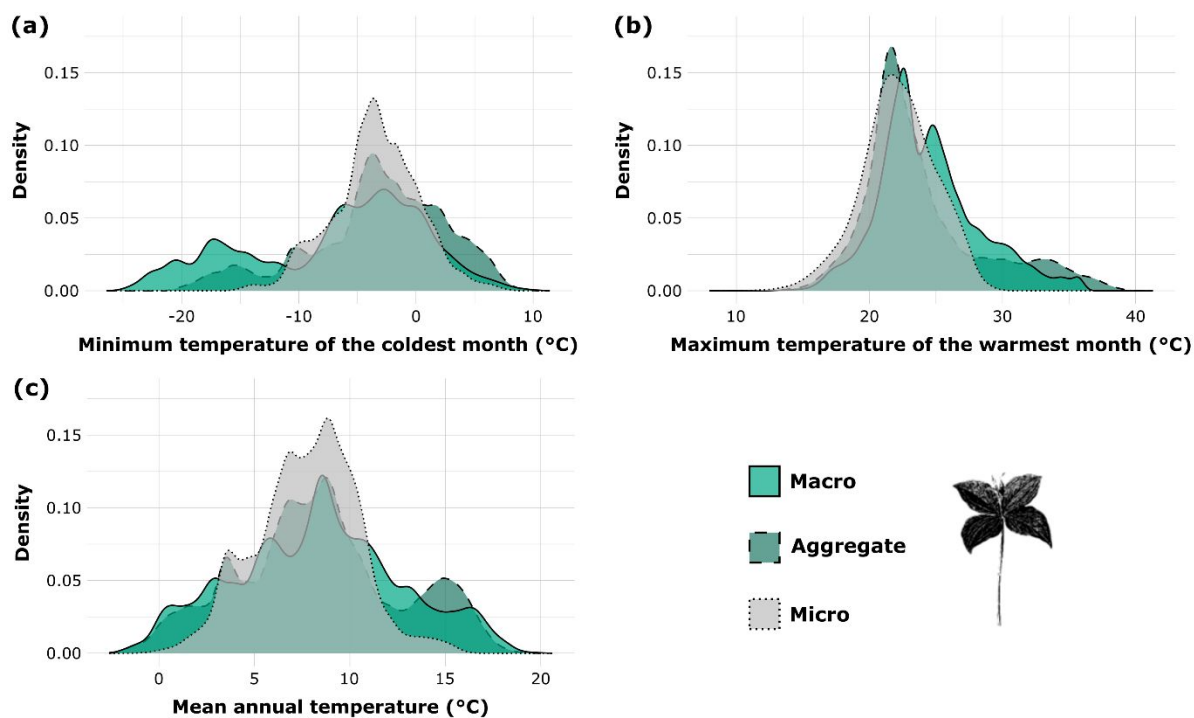


Figure 3: Pairwise comparison of the northern edge, southern edge, latitudinal range and potential suitable area, respectively between SDMs build with macroclimatic, aggregated microclimatic and microclimatic data. A positive effect size of the comparison reflects more northern latitudinal limits (at the northern and/or southern edge), higher latitudinal ranges and more potentially suitable area in SDMs built with the first group of climate data compared to the second group of climate data. Negative effect sizes reflect the opposite result. Points and associated black error bars correspond to posterior means and 95% highest posterior density intervals of the differences (of the standardized variables). Significant differences are indicated by solid dots whereas non-significant differences are indicated by transparent dots.

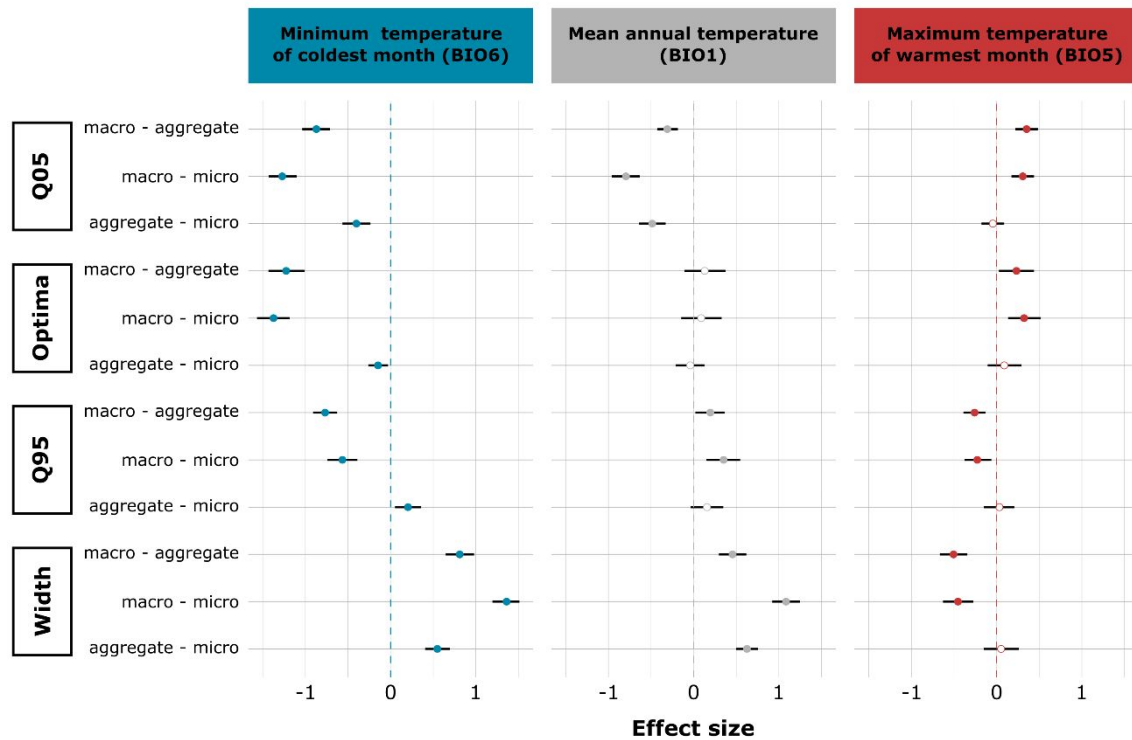
340 Species response curves

341 A first visual assessment of the response curves showed that microclimate-based response curves of
 342 minimum temperature of the coldest month, mean annual temperature and maximum temperature
 343 of the warmest month have different optima, and narrower niches compared to macroclimate-based
 344 response curves (e.g., *Paris quadrifolia*; Figure 4).



345
 346 *Figure 4: Species response curves for (a) minimum temperature of the coldest month, (b) maximum temperature*
 347 *of the warmest month and (c) mean annual temperature for Paris quadrifolia, illustrating the buffering effect*
 348 *that forest could exert on the thermal niche of species. Here, minimum temperatures are buffered at the cold*
 349 *edge of the response curve, whereas maximum temperatures are buffered at the warm edge of the response*
 350 *curve.*

351 Bayesian regression models showed that, for all modelled species, optima significantly differed
 352 between SDMs run with microclimate and macroclimate data for minimum and maximum
 353 temperatures, with warmer optima in minimum temperature and cooler optima in maximum
 354 temperature for microclimate-based SDMs relative to macroclimate based SDMs (Figure 5). However,
 355 for mean temperature there were no significant differences in optima between the different climate
 356 types. Furthermore, the niche width was narrower in minimum and mean temperatures for
 357 microclimate-based SDMs relative to macroclimate based SDMs. Surprisingly, the niche width was
 358 significantly wider in maximum temperatures for microclimate-based SDMs relative to macroclimate
 359 based SDMs.



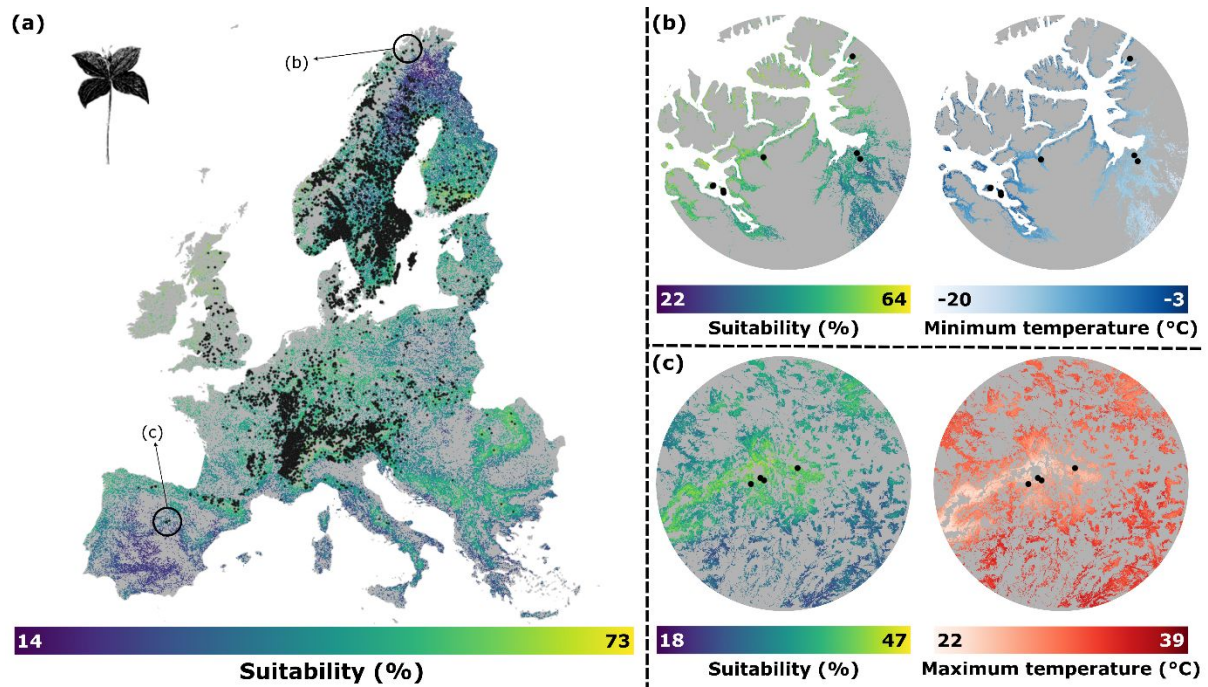
360

361 *Figure 5: Pairwise comparison of the cold edge (Q05), optimum, warm edge (Q95) and niche width, respectively*
 362 *between SDMs build with macroclimatic, aggregated microclimatic and microclimatic data. Each of the*
 363 *comparisons is made for minimum temperature of the coldest month (BIO6), mean annual temperature (BIO1),*
 364 *and maximum temperature of the warmest month (BIO5), respectively. A positive effect size reflects warmer*
 365 *values for the cold edge, optima and warm edge as well as wider niche widths, respectively, in SDMs built with*
 366 *the first group of climate data compared to the second group of climate data. Negative effect sizes reflect the*
 367 *opposite result. Points and associated black error bars correspond to posterior means and 95% highest posterior*
 368 *density intervals of the differences (of the standardized variables). Significant differences are indicated by solid*
 369 *dots whereas non-significant differences are indicated by transparent dots.*

370

Microrefugia

371 We found that 66% of all studied species are constrained to local microrefugia at their range limits.
 372 More specifically, 41% of the species occur in warm refugia relative to the surrounding landscape, at
 373 the northern limit of their latitudinal while 49% of the modelled species occur as remnant populations
 374 in cool refugia relative to the surrounding landscape, at the southern limit of their latitudinal range
 375 (e.g., *Paris quadrifolia*; Figure 6).



376

377 Figure 6: (a) Suitability map for *Paris quadrifolia* resulting from an SDM built with microclimatic data at 25×25
 378 m^2 resolution. The black dots represent the occurrence points extracted from GBIF and used as an input to the
 379 SDMs. We see that the species can occur in (b) warm refugia (i.e., higher minimum temperature values in the
 380 coldest month of the year) at its northern latitudinal limit and in (c) cool refugia (i.e., lower maximum
 381 temperature values in the warmest month of the year) at its southern latitudinal limit. The grey background
 382 shows non-forest areas.

DISCUSSION

Over the last years, microclimate research focused on improving our understanding of the drivers behind the differences between microclimate and macroclimate temperatures (Zellweger et al., 2019) and predicting and mapping microclimate temperatures across space and time (Greiser et al., 2018; Kearney et al., 2020). Although the drivers behind forest microclimates are relatively well understood, testing how microclimate layers perform within ecological applications such as SDMs has been limited, especially so across large (e.g., continental) spatial extents. However, with the recent advent of sub-canopy microclimate layers for European forests at $25 \times 25 \text{ m}^2$ resolution, a new avenue of species distribution modelling can be explored (Haesen et al., 2023). We found substantial differences in the model performance (based on the Continuous Boyce Index), indicating that microclimate-based SDMs significantly outperformed their conventional (i.e., macroclimate) counterparts and that aggregating microclimate data at coarser spatial resolutions leads to significant loss in model performance. Importantly, the use of aggregated microclimate data was still a significant improvement over the use of conventional macroclimate data in SDMs, which is especially interesting when computational capacity is limited. Our results thus agree with previous research reporting an increased performance of microclimate-based SDMs on regional scales (Ashcroft et al., 2008; Slavich et al., 2014; Stark & Fridley, 2022). However, this study additionally shows significant alterations of the species response curves to temperatures fitted with microclimatic data at a finer spatial resolution, matching the scale of the studied organisms (i.e., understory plants) more closely. This particular finding represents a major scientific advance with important implications in terms of SDMs' abilities to capture physiological processes that better reflect individual fitness.

We found significant differences in the shape of the species response curves obtained from the model predictions using different temperature sources. These outcomes underscore the importance of integrating microclimate data into SDMs, as previously proposed by Lembrechts et al. (2019). The recent increased availability of microclimatic data products at fine spatial resolution that cover large spatial extents has enabled us to uncover the true realized thermal niches and reveal the environmental conditions that actually matter for species living close to the ground surface (such as tree seedlings and herbaceous plants growing in the shade of trees). We demonstrate that species response curves derived from conventional macroclimate-based SDMs are much wider than one would expect given the buffering effect of forests (De Frenne et al., 2019; Harwood et al., 2014). Conventional SDMs might thus capture spurious correlations and fail to encompass the genuine factors constraining species distributions. The optima of the species response curves to maximum and minimum temperatures systematically shifted towards colder and warmer conditions, respectively, when using microclimate-based SDMs at fine spatial resolution, suggesting significant improvements

1
2
3 417 in SDMs' abilities to capture plant individual fitness in the forest understory. The same argument
4
5 418 applies to the species' thermal tolerance limits as we found systematic shifts towards warmer
6
7 419 conditions for the cold and warm tolerance limits of forest understory plants when using
8
9 420 microclimate-based SDMs at fine spatial resolution. The ability of microclimate-informed SDMs to
10
11 421 more accurately capture thermal tolerance limits holds important implications for exploring broader
12
13 422 macrophysiological thermal response patterns and organismal processes (Lancaster & Humphreys,
14
15 423 2020; Sentinella et al., 2020; Sunday et al., 2012). This capability could further advance the research
16
17 424 domain, aiding in the enhanced comprehension of plants' thermal safety margins in the face of climate
18
19 425 change, which are intricately tied to their survival, productivity, and reproductive capacities (Lancaster
20
21 426 & Humphreys, 2020).

22
23 427 Wider niches estimated by macroclimate-based SDMs also resulted in an overestimation of
24
25 428 the predicted range sizes, thereby confirming our second hypothesis. Indeed, the occurrence of a
26
27 429 species' individual within a specific macroclimatic pixel does not guarantee that the species will occur
28
29 430 in all other macroclimatic pixels with the same temperature because of considerable variations in
30
31 431 microclimate heterogeneity. This is especially important at range edges, where species will be found
32
33 432 in macroclimate pixels with above-average microclimate heterogeneity. Indeed, the populations of
34
35 433 66% of the studied species at the northern and southern limits of their latitudinal range are confined
36
37 434 to warm or cold spots in the landscape, respectively (Figure 6; Figure S2). Microclimate-based SDMs
38
39 435 thus allow for better identification of local microrefugia. Current macroclimate-based SDM practices
40
41 436 are unable to identify these microrefugia correctly as conventional macroclimate data represent the
42
43 437 overarching free-air temperatures rather than the local temperatures as perceived by organisms living
44
45 438 inside these microrefugia (Lenoir et al., 2017). Given the importance of microrefugia regarding the
46
47 439 accumulation and conservation of biodiversity (Finocchiaro et al., 2023; Nadeau et al., 2022), forest
48
49 440 management practices should be optimized to protect local microclimates and increase the capacity
50
51 441 of species and communities to resist to climate change (Hylander et al., 2022).

52
53 442 There are various reasons for the increased performance of microclimate-based SDMs, which
54
55 443 mainly relate to characteristics of the two primary input sources of each SDM: the occurrence points
56
57 444 and predictor variables. First, each occurrence point is subjected to a certain amount of positional
58
59 445 error (Wüest et al., 2020). In this study, we exclusively used records with a reported coordinate
60
446 uncertainty below 25 m. Nevertheless, applying a threshold on the positional error like this may induce
447
448 a loss of model performance by decreasing the number of occurrence points (Guisan et al., 2007).
449
450 Thus, it is conventionally recommended to decrease the spatial resolution of the analysis to account
451
452 for any positional errors in the occurrence points, rather than excluding the less precise records.
453
454 However, SDMs are sensitive to changes in the spatial resolution (Chauvier et al., 2022; Manzoor et

1
2
3 451 al., 2018). Decreasing spatial resolution inherently induces a loss of information as the data is
4
5 452 smoothed (i.e., aggregated), which comes at the cost of model performance as shown by the CBI
6
7 453 values from the models built with aggregated microclimatic data. Therefore, recent research strongly
8
9 454 recommends to fit SDMs as close as possible to the spatial grain that matches the biology of the focal
10
11 455 species (Gábor et al., 2022), meaning that it is recommended to calibrate SDMs with environmental
12
13 456 data consistent with the biological scale of the system or organism under study (Randin et al., 2009).
14
15 457 For instance, when modelling sessile species (i.e., species with limited mobility) or organisms in
16
17 458 ecosystems with high environmental heterogeneity, higher-resolution predictors are essential to
18
19 459 more precisely capture the intricacies of their niches (Norberg et al., 2019). For example, sessile
20
21 460 species are more prone to microclimate limitations due to their inability to actively relocate, rendering
22
23 461 them highly sensitive to variability in local environmental conditions and more likely to be spatially
24
25 462 limited to habitats with a particular microclimate. As a result, we anticipate that the findings of this
26
27 463 study may not be readily transferable when studying mobile species (such as birds or mammals) or
28
29 464 uniform environments.

30
31 465 Although promising, microclimate-based SDMs inherently face challenges beyond just
32
33 466 microclimate considerations. Analogous to other correlative climate-based SDMs, they are likely to
34
35 467 fail for many reasons unrelated to the accuracy and resolution of the climate data. For example, SDMs
36
37 468 often do not consider demographic processes and biotic interactions that mediate population
38
39 469 responses (Sanczuk et al., 2023). However, the SDM toolbox has been extended to accommodate
40
41 470 these shortcomings. For instance, range dynamic models explicitly consider demographic processes
42
43 471 such as dispersal and population dynamics (Zurell et al., 2016) and joint SDMs infer species
44
45 472 interactions from co-occurrence data (Ovaskainen & Abrego, 2020). Genomics-informed SDMs aiming
46
47 473 at including adaptability and demographic processes also offer interesting research avenues (Hudson
48
49 474 et al., 2021). Additionally, many SDMs do not include the fine-grained spatial heterogeneity of soil
50
51 475 conditions that may occur across few meters and which matter for species distributions (Beauregard
52
53 476 & de Blois, 2014; Buri et al., 2017; Roe et al., 2022). Disregarding the edaphic dimension in SDMs may
54
55 477 lead to overestimating the species' potential distribution as well as underestimating its spatial
56
57 478 fragmentation with important implications under anthropogenic climate change (Bertrand et al.,
58
59 479 2012).

60
61 480 Gridded microclimatic data at a resolution of $25 \times 25 \text{ m}^2$ are currently restricted to European
62
63 481 forests, which limits this study to 140 forest specialist plant species that exclusively live in forests
64
65 482 throughout their range. Herbaceous plant species living in open habitats, such as grasslands or
66
67 483 heathlands, are not included, as gridded microclimate data with the necessary spatial resolution is not
68
69 484 currently available for these environments at continental scale. The main reason for this is that

1
2
3 485 temperature sensors in open ecosystems are highly exposed to direct solar radiation, leading to
4
5 486 significant errors in the measurements recorded by the microclimate loggers (Maclean et al., 2021).
6
7 487 Consequently, the development of accurate microclimatic grids for these habitats is hindered.
8
9 488 Alternatively, mechanistic models that provided fine-grained gridded data products over large spatial
10
11 489 extents could also be used, but they are still missing because of computational challenges (Maclean,
12
13 490 2020). Nevertheless, accurate microclimate data over large spatial extents in open systems are
14
15 491 urgently needed to assess the transferability of the results from this study to a wider range of species.
16
17 492 Finally, while current microclimate products allow improved predictions of current species
18
19 493 distributions, microclimatic data predicted under future shared socioeconomic pathways (SSPs) are
20
21 494 needed to assess the impact of microclimate change on species ranges or the composition of species
22
23 495 communities (Lembrechts, 2023). However, forests are dynamic systems and their structural
24
25 496 characteristics that influence the forest microclimate cannot be assumed to remain constant over
26
27 497 time, making the development of such products challenging (De Lombaerde et al., 2022; Lenoir et al.,
28
29 498 2017). In a warming world, disturbances affecting forest canopies (e.g., drought, pests, storms) will
30
31 499 become more frequent and pronounced, drastically affecting the sub-canopy microclimate drastically
32
33 500 (Carlson et al., 2021; Kopáček et al., 2020; Thom et al., 2020). Given that many forest specialist species
34
35 501 have slow dispersal rates, often only several meters per year (Hermý et al., 1999; Svenning et al.,
36
37 502 2008), accurately evaluating their distribution ranges becomes crucial. It is very unlikely that these
38
39 503 species will be able to keep pace with contemporary macroclimate warming, wherein climate zones
40
41 504 are shifting several kilometres each year along the latitudinal gradient (Burrows et al., 2011). In this
42
43 505 regard, microclimate-based SDMs may allow us to accurately assess the velocity of microclimate
44
45 506 warming experienced by organisms in their immediate habitats and identify the locations where
46
47 507 species may become impacted due to climate change. While not explored in this study, this approach
48
49 508 could potentially reveal that microclimate heterogeneity mitigates the impact of climate change
50
51 509 (Maclean & Early, 2023), and therefore presents opportunities and obvious priorities for area-based
52
53 510 conservation.
54
55
56
57
58
59
60

1
2
3 511 **CONCLUSIONS**
4

5 512 To summarize, our study highlights the significant benefits of including microclimatic data in species
6 513 distribution models for forest plant species. By using microclimate-based SDMs, we were able to
7 514 uncover the hidden niche of forest plants, providing insights into their tolerance limits in response to
8 515 climate warming. This is in contrast to macroclimatic data, which estimated broader niches and could
9 516 not identify warm and cold refugia at the range edges of species distributions. Microclimate-based
10 517 SDMs are therefore essential for biodiversity conservation in the face of climate change, by providing
11 518 insights to optimize management actions and prioritize conservation efforts, particularly given the
12 519 growing policy and management focus on conservation of refugia worldwide.
13
14
15
16
17
18
19
20
21
22
23
24
25
26
27
28
29
30
31
32
33
34
35
36
37
38
39
40
41
42
43
44
45
46
47
48
49
50
51
52
53
54
55
56
57
58
59
60

For Review Only

520 ACKNOWLEDGEMENTS

521 This work was funded by Internal Funds of KU Leuven, an FWO Research Network Grant to SoilTemp
522 (W001919N) and the COST Action CA18201 – ConservePlants. SH was supported by a FLOF fellowship
523 (project nr. 3E190655) of the KU Leuven. JL received funding from: (i) the Agence Nationale de la
524 Recherche (ANR) (project IMPRINT; <https://microclimat.cnrs.fr>; grant nr. ANR-19-CE32-0005-01); (ii)
525 the Centre National de la Recherche Scientifique (CNRS) through the MITI interdisciplinary programs
526 (Défi INFINITI 2018: MORFO); (iii) and the Structure Fédérative de Recherche (SFR) Condorcet (FR CNRS
527 3417: CREUSE). JLL is funded by the Research Foundation Flanders (12P1819N) and by the ASICS
528 project (ANR-20-EBI5-0004, BiodivERsA, BiodivClim call 2019–2020). The study was also supported by
529 the Czech Science Foundation (project GACR 20-28119S) and the Czech Academy of Sciences (project
530 RVO 67985939). ChatGPT was used to improve English grammar and flow of the text.

531 REFERENCES

- 532 Ashcroft, M. B., Chisholm, L. A., & French, K. O. (2008). The effect of exposure on landscape scale soil
533 surface temperatures and species distribution models. *Landscape Ecology*, 23(2), 211–225.
534 <https://doi.org/10.1007/s10980-007-9181-8>
- 535 Beauregard, F., & de Blois, S. (2014). Beyond a Climate-Centric View of Plant Distribution: Edaphic
536 Variables Add Value to Distribution Models. *PLoS ONE*, 9(3), e92642.
537 <https://doi.org/10.1371/journal.pone.0092642>
- 538 Benito, B. M., Cayuela, L., & Albuquerque, F. S. (2013). The impact of modelling choices in the
539 predictive performance of richness maps derived from species-distribution models: guidelines to
540 build better diversity models. *Methods in Ecology and Evolution*, 4(4), 327–335.
541 <https://doi.org/10.1111/2041-210x.12022>
- 542 Bertrand, R., Perez, V., & Gégout, J.-C. (2012). Disregarding the edaphic dimension in species
543 distribution models leads to the omission of crucial spatial information under climate change:
544 the case of *Quercus pubescens* in France. *Global Change Biology*, 18(8), 2648–2660.
545 <https://doi.org/10.1111/j.1365-2486.2012.02679.x>
- 546 Booth, T. H. (2022). Checking bioclimatic variables that combine temperature and precipitation data
547 before their use in species distribution models. *Austral Ecology*, 47(7), 1506–1514.
548 <https://doi.org/10.1111/aec.13234>

- 1
2
3 549 Booth, T. H., Nix, H. A., Busby, J. R., & Hutchinson, M. F. (2014). bioclim: the first species distribution
4 550 modelling package, its early applications and relevance to most current MaxEnt studies. *Diversity*
5 551 *and Distributions*, 20(1), 1–9. <https://doi.org/10.1111/ddi.12144>
6
7
8
9 552 Buri, A., Cianfrani, C., Pinto-Figueroa, E., Yashiro, E., Spangenberg, J. E., Adatte, T., Verrecchia, E.,
10 553 Guisan, A., & Pradervand, J.-N. (2017). Soil factors improve predictions of plant species
11 554 distribution in a mountain environment. *Progress in Physical Geography: Earth and Environment*,
12 555 41(6), 703–722. <https://doi.org/10.1177/0309133317738162>
13
14
15
16 556 Bürkner, P.-C. (2021). Bayesian Item Response Modeling in R with brms and Stan. *Journal of Statistical*
17 557 *Software*, 100(5). <https://doi.org/10.18637/jss.v100.i05>
18
19
20 558 Burnham, K. P., & Anderson, D. R. (2004). Multimodel Inference. *Sociological Methods & Research*,
21 559 33(2), 261–304. <https://doi.org/10.1177/0049124104268644>
22
23
24 560 Burrows, M. T., Schoeman, D. S., Buckley, L. B., Moore, P., Poloczanska, E. S., Brander, K. M., Brown,
25 561 C., Bruno, J. F., Duarte, C. M., Halpern, B. S., Holding, J., Kappel, C. V., Kiessling, W., O'Connor, M.
26 562 I., Pandolfi, J. M., Parmesan, C., Schwing, F. B., Sydeman, W. J., & Richardson, A. J. (2011). The
27 563 Pace of Shifting Climate in Marine and Terrestrial Ecosystems. *Science*, 334(6056), 652–655.
28 564 <https://doi.org/10.1126/science.1210288>
29
30
31
32
33 565 Carlson, A. R., Sibold, J. S., & Negrón, J. F. (2021). Wildfire and spruce beetle outbreak have mixed
34 566 effects on below-canopy temperatures in a Rocky Mountain subalpine forest. *Journal of*
35 567 *Biogeography*, 48(1), 216–230. <https://doi.org/10.1111/jbi.13994>
36
37
38
39 568 Caron, M. M., Zellweger, F., Verheyen, K., Baeten, L., Hédli, R., Bernhardt-Römermann, M., Berki, I.,
40 569 Brunet, J., Decocq, G., Díaz, S., Dirnböck, T., Durak, T., Heinken, T., Jaroszewicz, B., Kopecký, M.,
41 570 Lenoir, J., Macek, M., Malicki, M., Máliš, F., ... De Frenne, P. (2021). Thermal differences between
42 571 juveniles and adults increased over time in European forest trees. *Journal of Ecology*, 109(11),
43 572 3944–3957. <https://doi.org/10.1111/1365-2745.13773>
44
45
46
47
48 573 Chauvier, Y., Descombes, P., Guéguen, M., Boulangeat, L., Thuiller, W., & Zimmermann, N. E. (2022).
49 574 Resolution in species distribution models shapes spatial patterns of plant multifaceted diversity.
50 575 *Ecography*, 2022(10). <https://doi.org/10.1111/ecog.05973>
51
52
53
54 576 Cheng, Y., Tjaden, N. B., Jaeschke, A., Thomas, S. M., & Beierkuhnlein, C. (2021). Using centroids of
55 577 spatial units in ecological niche modelling: Effects on model performance in the context of
56 578 environmental data grain size. *Global Ecology and Biogeography*, 30(3), 611–621.
57 579 <https://doi.org/10.1111/geb.13240>
58
59
60

- 1
2
3 580 De Frenne, P., Zellweger, F., Rodríguez-Sánchez, F., Scheffers, B. R., Hylander, K., Luoto, M., Vellend,
4 581 M., Verheyen, K., & Lenoir, J. (2019). Global buffering of temperatures under forest canopies.
5 582 *Nature Ecology & Evolution*, 3(5), 744–749. <https://doi.org/10.1038/s41559-019-0842-1>
6
7
8
9 583 De Lombaerde, E., Vangansbeke, P., Lenoir, J., Van Meerbeek, K., Lembrechts, J., Rodríguez-Sánchez,
10 584 F., Luoto, M., Scheffers, B., Haesen, S., Aalto, J., Christiansen, D. M., De Pauw, K., Depauw, L.,
11 585 Govaert, S., Greiser, C., Hampe, A., Hylander, K., Klings, D., Koelemeijer, I., ... De Frenne, P.
12 586 (2022). Maintaining forest cover to enhance temperature buffering under future climate change.
13 587 *Science of The Total Environment*, 810, 151338.
14 588 <https://doi.org/10.1016/j.scitotenv.2021.151338>
15
16
17
18
19 589 Dobrowski, S. Z. (2011). A climatic basis for microrefugia: the influence of terrain on climate. *Global*
20 590 *Change Biology*, 17(2), 1022–1035. <https://doi.org/10.1111/j.1365-2486.2010.02263.x>
21
22
23 591 Dormann, C. F., Elith, J., Bacher, S., Buchmann, C., Carl, G., Carré, G., Marquéz, J. R. G., Gruber, B.,
24 592 Lafourcade, B., Leitão, P. J., Münkemüller, T., McClean, C., Osborne, P. E., Reineking, B., Schröder,
25 593 B., Skidmore, A. K., Zurell, D., & Lautenbach, S. (2013). Collinearity: a review of methods to deal
26 594 with it and a simulation study evaluating their performance. *Ecography*, 36(1), 27–46.
27 595 <https://doi.org/10.1111/j.1600-0587.2012.07348.x>
28
29
30
31
32 596 Elith, J., & Leathwick, J. R. (2009). Species Distribution Models: Ecological Explanation and Prediction
33 597 Across Space and Time. *Annual Review of Ecology, Evolution, and Systematics*, 40(1), 677–697.
34 598 <https://doi.org/10.1146/annurev.ecolsys.110308.120159>
35
36
37
38 599 Fick, S. E., & Hijmans, R. J. (2017). WorldClim 2: new 1-km spatial resolution climate surfaces for global
39 600 land areas. *International Journal of Climatology*, 37(12), 4302–4315.
40 601 <https://doi.org/10.1002/joc.5086>
41
42
43
44 602 Finocchiaro, M., Médail, F., Saatkamp, A., Diadema, K., Pavon, D., & Meineri, E. (2023). Bridging the
45 603 gap between microclimate and microrefugia: A bottom-up approach reveals strong climatic and
46 604 biological offsets. *Global Change Biology*, 29(4), 1024–1036. <https://doi.org/10.1111/gcb.16526>
47
48
49
50 605 Fourcade, Y., Besnard, A. G., & Secondi, J. (2018). Paintings predict the distribution of species, or the
51 606 challenge of selecting environmental predictors and evaluation statistics. *Global Ecology and*
52 607 *Biogeography*, 27(2), 245–256. <https://doi.org/10.1111/geb.12684>
53
54
55 608 Gábor, L., Jetz, W., Lu, M., Rocchini, D., Cord, A., Malavasi, M., Zarzo-Arias, A., Barták, V., & Moudrý,
56 609 V. (2022). Positional errors in species distribution modelling are not overcome by the coarser
57
58
59
60

- 1
2
3 610 grains of analysis. *Methods in Ecology and Evolution*, 13(10), 2289–2302.
4
5 611 <https://doi.org/10.1111/2041-210X.13956>
6
7 612 Geiger, R. (1950). *The climate near the ground*. Cambridge, Mass.: Harvard University Press. 482p.
8
9 613 pages.
10
11 614 Greiser, C., Meineri, E., Luoto, M., Ehrlén, J., & Hylander, K. (2018). Monthly microclimate models in a
12 managed boreal forest landscape. *Agricultural and Forest Meteorology*, 250–251, 147–158.
13 615 <https://doi.org/10.1016/j.agrformet.2017.12.252>
14 616
15
16 617 Guisan, A., Graham, C. H., Elith, J., & Huettmann, F. (2007). Sensitivity of predictive species distribution
18 models to change in grain size. *Diversity and Distributions*, 13(3), 332–340.
19 618 <https://doi.org/10.1111/j.1472-4642.2007.00342.x>
20 619
21
22 620 Guisan, A., & Zimmermann, N. E. (2000). Predictive habitat distribution models in ecology. *Ecological*
23 621 *Modelling*, 135(2–3), 147–186. [https://doi.org/10.1016/S0304-3800\(00\)00354-9](https://doi.org/10.1016/S0304-3800(00)00354-9)
24 622
25
26 622 Haesen, S., Lembrechts, J. J., De Frenne, P., Lenoir, J., Aalto, J., Ashcroft, M. B., Kopecký, M., Luoto, M.,
28 623 Maclean, I., Nijs, I., Niittynen, P., Hoogen, J., Arriga, N., Brůna, J., Buchmann, N., Čiliak, M.,
29 624 Collalti, A., De Lombaerde, E., Descombes, P., ... Van Meerbeek, K. (2021). ForestTemp –
31 625 Sub-canopy microclimate temperatures of European forests. *Global Change Biology*, 27(23),
32 626 6307–6319. <https://doi.org/10.1111/gcb.15892>
33 627
34
35 627 Haesen, S., Lembrechts, J. J., De Frenne, P., Lenoir, J., Aalto, J., Ashcroft, M. B., Kopecký, M., Luoto, M.,
37 628 Maclean, I., Nijs, I., Niittynen, P., van den Hoogen, J., Arriga, N., Brůna, J., Buchmann, N., Čiliak,
38 629 M., Collalti, A., De Lombaerde, E., Descombes, P., ... Van Meerbeek, K. (2023). ForestClim —
40 630 Bioclimatic variables for microclimate temperatures of European forests. *Global Change Biology*,
41 631 29(11), 2886–2892. <https://doi.org/10.1111/gcb.16678>
42 632
43
44 632 Hageer, Y., Esperón-Rodríguez, M., Baumgartner, J. B., & Beaumont, L. J. (2017). Climate, soil or both?
46 633 Which variables are better predictors of the distributions of Australian shrub species? *PeerJ*, 5(6),
47 634 e3446. <https://doi.org/10.7717/peerj.3446>
48 635
49
50 635 Harwood, T. D., Mokany, K., & Paini, D. R. (2014). Microclimate is integral to the modeling of plant
51 636 responses to macroclimate. *Proceedings of the National Academy of Sciences*, 111(13).
52 637 <https://doi.org/10.1073/pnas.1400069111>
53 638
54
55 638 Heinken, T., Diekmann, M., Liira, J., Orczewska, A., Schmidt, M., Brunet, J., Chytrý, M., Chabrierie, O.,
57 639 Decocq, G., De Frenne, P., Dřevojan, P., Dzwonko, Z., Ewald, J., Feilberg, J., Graae, B. J., Grytnes,
58 640 J., Hermy, M., Kriebitzsch, W., Laiviņš, M., ... Vanneste, T. (2022). The European Forest Plant

- 1
2
3 641 Species List (EuForPlant): Concept and applications. *Journal of Vegetation Science*, 33(3).
4
5 642 <https://doi.org/10.1111/jvs.13132>
6
7 643 Hermy, M., Honnay, O., Firbank, L., Grashof-Bokdam, C., & Lawesson, J. E. (1999). An ecological
8
9 644 comparison between ancient and other forest plant species of Europe, and the implications for
10
11 645 forest conservation. *Biological Conservation*, 91(1), 9–22. <https://doi.org/10.1016/S0006->
12
13 646 3207(99)00045-2
14
15 647 Hirzel, A. H., Le Lay, G., Helfer, V., Randin, C., & Guisan, A. (2006). Evaluating the ability of habitat
16
17 648 suitability models to predict species presences. *Ecological Modelling*, 199(2), 142–152.
18
19 649 <https://doi.org/10.1016/j.ecolmodel.2006.05.017>
20
21 650 Hudson, J., Castilla, J. C., Teske, P. R., Beheregaray, L. B., Haigh, I. D., McQuaid, C. D., & Rius, M. (2021).
22
23 651 Genomics-informed models reveal extensive stretches of coastline under threat by an
24
25 652 ecologically dominant invasive species. *Proceedings of the National Academy of Sciences*,
26
27 653 118(23), e2022169118. <https://doi.org/10.1073/pnas.2022169118>
28
29 654 Hylander, K., Greiser, C., Christiansen, D. M., & Koelemeijer, I. A. (2022). Climate adaptation of
30
31 655 biodiversity conservation in managed forest landscapes. *Conservation Biology*, 36(3), e13847.
32
33 656 <https://doi.org/10.1111/cobi.13847>
34
35 657 Jarraud, M. (2008). *Guide to meteorological instruments and methods of observation (WMO-No. 8)*.
36
37 658 Jiménez, L., & Soberón, J. (2020). Leaving the area under the receiving operating characteristic curve
38
39 659 behind: An evaluation method for species distribution modelling applications based on
40
41 660 presence-only data. *Methods in Ecology and Evolution*, 11(12), 1571–1586.
42
43 661 <https://doi.org/10.1111/2041-210X.13479>
44
45 662 Karger, D. N., Conrad, O., Böhrner, J., Kawohl, T., Kreft, H., Soria-Auza, R. W., Zimmermann, N. E., Linder,
46
47 663 H. P., & Kessler, M. (2017). Climatologies at high resolution for the earth's land surface areas.
48
49 664 *Scientific Data*, 4(1), 170122. <https://doi.org/10.1038/sdata.2017.122>
50
51 665 Kass, J. M., Muscarella, R., Galante, P. J., Bohl, C. L., Pinilla-Buitrago, G. E., Boria, R. A., Soley-Guardia,
52
53 666 M., & Anderson, R. P. (2021). ENMeval 2.0: Redesigned for customizable and reproducible
54
55 667 modeling of species' niches and distributions. *Methods in Ecology and Evolution*, 12(9), 1602–
56
57 668 1608. <https://doi.org/10.1111/2041-210X.13628>
58
59 669 Kearney, M. R., Gillingham, P. K., Bramer, I., Duffy, J. P., & Maclean, I. M. D. (2020). A method for
60
61 670 computing hourly, historical, terrain-corrected microclimate anywhere on earth. *Methods in*
62
63 671 *Ecology and Evolution*, 11(1), 38–43. <https://doi.org/10.1111/2041-210X.13330>

- 1
2
3 672 Kopáček, J., Bače, R., Hejzlar, J., Kaňa, J., Kučera, T., Matějka, K., Porcal, P., & Turek, J. (2020). Changes
4 673 in microclimate and hydrology in an unmanaged mountain forest catchment after insect-induced
5 674 tree dieback. *Science of The Total Environment*, 720, 137518.
6 675 <https://doi.org/10.1016/j.scitotenv.2020.137518>
7
8
9
10 676 Körner, C., & Hiltbrunner, E. (2018). The 90 ways to describe plant temperature. *Perspectives in Plant*
11 677 *Ecology, Evolution and Systematics*, 30, 16–21. <https://doi.org/10.1016/j.ppees.2017.04.004>
12
13
14 678 Lake, T. A., Briscoe Runquist, R. D., & Moeller, D. A. (2020). Predicting range expansion of invasive
15 679 species: Pitfalls and best practices for obtaining biologically realistic projections. *Diversity and*
16 680 *Distributions*, 26(12), 1767–1779. <https://doi.org/10.1111/ddi.13161>
17
18
19
20 681 Lancaster, L. T., & Humphreys, A. M. (2020). Global variation in the thermal tolerances of plants.
21 682 *Proceedings of the National Academy of Sciences*, 117(24), 13580–13587.
22 683 <https://doi.org/10.1073/pnas.1918162117>
23
24
25
26 684 Lembrechts, J. J. (2023). Microclimate alters the picture. *Nature Climate Change*, 13(5), 423–424.
27 685 <https://doi.org/10.1038/s41558-023-01632-5>
28
29
30 686 Lembrechts, J. J., Nijs, I., & Lenoir, J. (2019). Incorporating microclimate into species distribution
31 687 models. *Ecography*, 42(7), 1267–1279. <https://doi.org/10.1111/ecog.03947>
32
33
34 688 Lenoir, J., Hattab, T., & Pierre, G. (2017). Climatic microrefugia under anthropogenic climate change:
35 689 implications for species redistribution. *Ecography*, 40(2), 253–266.
36 690 <https://doi.org/10.1111/ecog.02788>
37
38
39
40 691 Lenth, R. V. (2021). *emmeans: Estimated Marginal Means, aka Least-Squares Means*.
41
42 692 Lozier, J. D., Aniello, P., & Hickerson, M. J. (2009). Predicting the distribution of Sasquatch in western
43 693 North America: anything goes with ecological niche modelling. *Journal of Biogeography*, 36(9),
44 694 1623–1627. <https://doi.org/10.1111/j.1365-2699.2009.02152.x>
45
46
47
48 695 Macek, M., Kopecký, M., & Wild, J. (2019). Maximum air temperature controlled by landscape
49 696 topography affects plant species composition in temperate forests. *Landscape Ecology*, 34(11),
50 697 2541–2556. <https://doi.org/10.1007/s10980-019-00903-x>
51
52
53
54 698 Maclean, I. M. D. (2020). Predicting future climate at high spatial and temporal resolution. *Global*
55 699 *Change Biology*, 26(2), 1003–1011. <https://doi.org/10.1111/gcb.14876>
56
57
58 700 Maclean, I. M. D., Duffy, J. P., Haesen, S., Govaert, S., De Frenne, P., Vanneste, T., Lenoir, J.,
59 701 Lembrechts, J. J., Rhodes, M. W., & Van Meerbeek, K. (2021). On the measurement of

- 1
2
3 702 microclimate. *Methods in Ecology and Evolution*, 12(8), 1397–1410.
4
5 703 <https://doi.org/10.1111/2041-210X.13627>
6
7 704 Maclean, I. M. D., & Early, R. (2023). Macroclimate data overestimate range shifts of plants in response
8
9 705 to climate change. *Nature Climate Change*, 13(5), 484–490. [https://doi.org/10.1038/s41558-](https://doi.org/10.1038/s41558-023-01650-3)
10 706 [023-01650-3](https://doi.org/10.1038/s41558-023-01650-3)
11
12
13 707 Man, M., Wild, J., Macek, M., & Kopecký, M. (2022). Can high-resolution topography and forest canopy
14
15 708 structure substitute microclimate measurements? Bryophytes say no. *Science of The Total*
16 709 *Environment*, 821, 153377. <https://doi.org/10.1016/j.scitotenv.2022.153377>
17
18
19 710 Manzoor, S. A., Griffiths, G., & Lukac, M. (2018). Species distribution model transferability and model
20 711 grain size – finer may not always be better. *Scientific Reports*, 8(1), 7168.
21 712 <https://doi.org/10.1038/s41598-018-25437-1>
22
23
24 713 Merow, C., Smith, M. J., & Silander, J. A. (2013). A practical guide to MaxEnt for modeling species'
25 714 distributions: what it does, and why inputs and settings matter. *Ecography*, 36(10), 1058–1069.
26 715 <https://doi.org/10.1111/j.1600-0587.2013.07872.x>
27
28
29
30 716 Muscarella, R., Galante, P. J., Soley-Guardia, M., Boria, R. A., Kass, J. M., Uriarte, M., & Anderson, R. P.
31 717 (2014). ENMeval: An R package for conducting spatially independent evaluations and estimating
32 718 optimal model complexity for Maxent ecological niche models. *Methods in Ecology and*
33 719 *Evolution*, 5(11), 1198–1205. <https://doi.org/10.1111/2041-210X.12261>
34
35
36
37 720 Nadeau, C. P., Giacomazzo, A., & Urban, M. C. (2022). Cool microrefugia accumulate and conserve
38 721 biodiversity under climate change. *Global Change Biology*, 28(10), 3222–3235.
39 722 <https://doi.org/10.1111/gcb.16143>
40
41
42
43 723 Norberg, A., Abrego, N., Blanchet, F. G., Adler, F. R., Anderson, B. J., Anttila, J., Araújo, M. B., Dallas,
44 724 T., Dunson, D., Elith, J., Foster, S. D., Fox, R., Franklin, J., Godsoe, W., Guisan, A., O'Hara, B., Hill,
45 725 N. A., Holt, R. D., Hui, F. K. C., ... Ovaskainen, O. (2019). A comprehensive evaluation of predictive
46 726 performance of 33 species distribution models at species and community levels. *Ecological*
47 727 *Monographs*, 89(3), e01370. <https://doi.org/10.1002/ecm.1370>
48
49
50
51
52 728 Ovaskainen, O., & Abrego, N. (2020). *Joint Species Distribution Modelling*. Cambridge University Press.
53 729 <https://doi.org/10.1017/9781108591720>
54
55
56 730 Phillips, S. J., Anderson, R. P., Dudík, M., Schapire, R. E., & Blair, M. E. (2017). Opening the black box:
57 731 an open-source release of Maxent. *Ecography*, 40(7), 887–893.
58 732 <https://doi.org/10.1111/ecog.03049>
59
60

- 1
2
3 733 Poggio, L., de Sousa, L. M., Batjes, N. H., Heuvelink, G. B. M., Kempen, B., Ribeiro, E., & Rossiter, D.
4
5 734 (2021). SoilGrids 2.0: producing soil information for the globe with quantified spatial uncertainty.
6
7 735 *SOIL*, 7(1), 217–240. <https://doi.org/10.5194/soil-7-217-2021>
- 8
9 736 R Core Team. (2021). *R: A Language and Environment for Statistical Computing*.
- 10
11 737 Radosavljevic, A., & Anderson, R. P. (2014). Making better Maxent models of species distributions:
12
13 738 complexity, overfitting and evaluation. *Journal of Biogeography*, 41(4), 629–643.
14
15 739 <https://doi.org/10.1111/jbi.12227>
- 16
17 740 Randin, C. F., Engler, R., Normand, S., Zappa, M., Zimmermann, N. E., Pearman, P. B., Vittoz, P., Thuiller,
18
19 741 W., & Guisan, A. (2009). Climate change and plant distribution: local models predict high-
20
21 742 elevation persistence. *Global Change Biology*, 15(6), 1557–1569.
22
23 743 <https://doi.org/10.1111/j.1365-2486.2008.01766.x>
- 24
25 744 Roe, N. A., Ducey, M. J., Lee, T. D., Fraser, O. L., Colter, R. A., & Hallett, R. A. (2022). Soil chemical
26
27 745 variables improve models of understorey plant species distributions. *Journal of Biogeography*,
28
29 746 49(4), 753–766. <https://doi.org/10.1111/jbi.14344>
- 30
31 747 Sanczuk, P., De Pauw, K., De Lombaerde, E., Luoto, M., Meeussen, C., Govaert, S., Vanneste, T.,
32
33 748 Depauw, L., Brunet, J., Cousins, S. A. O., Gasperini, C., Hedwall, P.-O., Iacopetti, G., Lenoir, J., Plue,
34
35 749 J., Selvi, F., Spicher, F., Uria-Diez, J., Verheyen, K., ... De Frenne, P. (2023). Microclimate and forest
36
37 750 density drive plant population dynamics under climate change. *Nature Climate Change*, 13(8),
38
39 751 840–847. <https://doi.org/10.1038/s41558-023-01744-y>
- 40
41 752 Sentinella, A. T., Warton, D. I., Sherwin, W. B., Offord, C. A., & Moles, A. T. (2020). Tropical plants do
42
43 753 not have narrower temperature tolerances, but are more at risk from warming because they are
44
45 754 close to their upper thermal limits. *Global Ecology and Biogeography*, 29(8), 1387–1398.
46
47 755 <https://doi.org/10.1111/geb.13117>
- 48
49 756 Slavich, E., Warton, D. I., Ashcroft, M. B., Gollan, J. R., & Ramp, D. (2014). Topoclimate versus
50
51 757 macroclimate: how does climate mapping methodology affect species distribution models and
52
53 758 climate change projections? *Diversity and Distributions*, 20(8), 952–963.
54
55 759 <https://doi.org/10.1111/ddi.12216>
- 56
57 760 Stark, J. R., & Fridley, J. D. (2022). Microclimate-based species distribution models in complex forested
58
59 761 terrain indicate widespread cryptic refugia under climate change. *Global Ecology and*
60
762 *Biogeography*, 31(3), 562–575. <https://doi.org/10.1111/geb.13447>

- 1
2
3 763 Sunday, J. M., Bates, A. E., & Dulvy, N. K. (2012). Thermal tolerance and the global redistribution
4 of animals. *Nature Climate Change*, 2(9), 686–690. <https://doi.org/10.1038/nclimate1539>
5 764
6
7 765 Svenning, J.-C., Normand, S., & Skov, F. (2008). Postglacial dispersal limitation of widespread forest
8 plant species in nemoral Europe. *Ecography*, 31(3), 316–326. <https://doi.org/10.1111/j.0906->
9 766
10 767 7590.2008.05206.x
11
12
13 768 Thom, D., Sommerfeld, A., Sebald, J., Hagge, J., Müller, J., & Seidl, R. (2020). Effects of disturbance
14 patterns and deadwood on the microclimate in European beech forests. *Agricultural and Forest*
15 769 *Meteorology*, 291, 108066. <https://doi.org/10.1016/j.agrformet.2020.108066>
16 770
17
18 771 van Proosdij, A. S. J., Sosef, M. S. M., Wieringa, J. J., & Raes, N. (2016). Minimum required number of
19 772 specimen records to develop accurate species distribution models. *Ecography*, 39(6), 542–552.
20 773 <https://doi.org/10.1111/ecog.01509>
21
22
23 774 Venables, W. N., & Ripley, B. D. (2002). *Modern Applied Statistics with S, Fourth edition*. Springer, New
24 775 York.
25
26
27
28 776 Wüest, R. O., Zimmermann, N. E., Zurell, D., Alexander, J. M., Fritz, S. A., Hof, C., Kreft, H., Normand,
29 777 S., Cabral, J. S., Szekely, E., Thuiller, W., Wikelski, M., & Karger, D. N. (2020). Macroecology in the
30 778 age of Big Data – Where to go from here? *Journal of Biogeography*, 47(1), 1–12.
31 779 <https://doi.org/10.1111/jbi.13633>
32
33
34
35 780 Zellweger, F., Coomes, D., Lenoir, J., Depauw, L., Maes, S. L., Wulf, M., Kirby, K. J., Brunet, J., Kopecký,
36 781 M., Máliš, F., Schmidt, W., Heinrichs, S., den Ouden, J., Jaroszewicz, B., Buyse, G., Spicher, F.,
37 782 Verheyen, K., & De Frenne, P. (2019). Seasonal drivers of understorey temperature buffering in
38 783 temperate deciduous forests across Europe. *Global Ecology and Biogeography*, 28(12), 1774–
39 784 1786. <https://doi.org/10.1111/geb.12991>
40
41
42
43
44 785 Zimmermann, N. E., Edwards, T. C., Graham, C. H., Pearman, P. B., & Svenning, J.-C. (2010). New trends
45 786 in species distribution modelling. *Ecography*, 33(6), 985–989. <https://doi.org/10.1111/j.1600->
46 787 0587.2010.06953.x
47
48
49
50 788 Zurell, D., Franklin, J., König, C., Bouchet, P. J., Dormann, C. F., Elith, J., Fandos, G., Feng, X.,
51 789 Guillera-Arroita, G., Guisan, A., Lahoz-Monfort, J. J., Leitão, P. J., Park, D. S., Peterson, A. T.,
52 790 Rapacciuolo, G., Schmatz, D. R., Schröder, B., Serra-Diaz, J. M., Thuiller, W., ... Merow, C. (2020).
53 791 A standard protocol for reporting species distribution models. *Ecography*, 43(9), 1261–1277.
54 792 <https://doi.org/10.1111/ecog.04960>
55
56
57
58
59
60

1
2
3 793 Zurell, D., Thuiller, W., Pagel, J., Cabral, J. S., Münkemüller, T., Gravel, D., Dullinger, S., Normand, S.,
4
5 794 Schiffers, K. H., Moore, K. A., & Zimmermann, N. E. (2016). Benchmarking novel approaches for
6
7 795 modelling species range dynamics. *Global Change Biology*, 22(8), 2651–2664.
8
9 796 <https://doi.org/10.1111/gcb.13251>

10 797
11
12
13
14
15
16
17
18
19
20
21
22
23
24
25
26
27
28
29
30
31
32
33
34
35
36
37
38
39
40
41
42
43
44
45
46
47
48
49
50
51
52
53
54
55
56
57
58
59
60

For Review Only